

**NASA Contractor Report 178421**

**ICASE REPORT NO. 87-74**

# ICASE

NUMERICAL SOLUTION OF TURBULENT FLOW PAST A  
BACKWARD FACING STEP USING A NONLINEAR K- $\epsilon$  MODEL

C. G. Speziale

Tuan Ngo

{NASA-CR-178421} - NUMERICAL SOLUTION OF  
TURBULENT FLOW PAST A BACKWARD FACING STEP  
USING A NONLINEAR K-EPSILON MODEL Final  
Report {NASA} 46 p CSCL 20D

N88-15189

G3/34 Unclass  
0119510

Contract No. NAS1-18107  
December 1987

INSTITUTE FOR COMPUTER APPLICATIONS IN SCIENCE AND ENGINEERING  
NASA Langley Research Center, Hampton, Virginia 23665

Operated by the Universities Space Research Association



National Aeronautics and  
Space Administration

**Langley Research Center**  
Hampton, Virginia 23665

# NUMERICAL SOLUTION OF TURBULENT FLOW PAST A BACKWARD FACING STEP USING A NONLINEAR K- $\epsilon$ MODEL

C. G. Speziale and Tuan Ngo

The George W. Woodruff School of Mechanical Engineering

Georgia Institute of Technology

Atlanta, GA 30332

## ABSTRACT

The problem of turbulent flow past a backward facing step is important in many technological applications and has been used as a standard test case to evaluate the performance of turbulence models in the prediction of separated flows. It is well known that the commonly used K- $\epsilon$  (and K- $l$ ) models of turbulence yield inaccurate predictions for the reattachment point in this problem. By an analysis of the mean vorticity transport equation, it will be argued that the intrinsically inaccurate prediction of normal Reynolds stress differences by the K- $\epsilon$  and K- $l$  models is a major contributor to this problem. Computations using a new nonlinear K- $\epsilon$  model (which alleviates this deficiency) are made with the TEACH program. Comparisons are made between the improved results predicted by this nonlinear K- $\epsilon$  model and those obtained from the linear K- $\epsilon$  model as well as from second-order closure models.

---

This research was supported by the National Aeronautics and Space Administration under NASA Contract No. NAS1-18107 while the first author was in residence at the Institute for Computer Applications in Science and Engineering (ICASE), NASA Langley Research Center, Hampton, VA 23665 and by the Office of Naval Research under Contract No. N00014-85-K-0238.



## 1. INTRODUCTION

Among the various turbulence models in existence, the linear  $K-\epsilon$  and  $K-\ell$  models are the most widely used by scientists and engineers to solve practical problems. The primary advantages of the models include their broad invariance properties and the relatively simple manner in which they can be incorporated into most existing Navier-Stokes computer codes which allow for a variable viscosity (see Speziale 1987). Furthermore, for unseparated turbulent boundary layers, these linear  $K-\ell$  and  $K-\epsilon$  models have been shown to provide excellent descriptions of the flow (see Rodi 1982).

However, one major drawback of the linear  $K-\epsilon$  (and  $K-\ell$ ) model is that it yields highly inaccurate predictions for the normal Reynolds stress differences. Consequently, for the types of turbulent flow where the normal Reynolds stress differences play an important role (such as secondary flows in a non-circular duct or separated flows), the linear models can give rise to considerable inaccuracies. There have been many efforts over the years to include nonlinear effects in the modeling of the Reynolds stresses within a two-equation format (see Lumley 1970, Launder and Ying 1971, Gessner and Emery 1976, and Saffman 1977). However, these models do not exhibit the general invariance necessary for the broadest range of application. Recently, a nonlinear  $K-\epsilon$  (and  $K-\ell$ ) model was obtained by making an asymptotic expansion subject to the constraints of dimensional and tensorial invariance, realizability, and material frame-indifference in the

limit of two-dimensional turbulence (see Speziale 1987). This model was shown to yield improved predictions for the normal Reynolds stresses in internal flows which are unseparated. However, for any proposed model to be sufficiently applicable, it has to be successful in predicting turbulent flows which have separated regions since these occur in a wide variety of problems which are of technological importance.

In this study, the new nonlinear  $K-\epsilon$  model is incorporated into the TEACH computer code in order to analyze the problem of a two-dimensional turbulent flow past a backward facing step. Turbulent flow past a backward facing step has served as a primary benchmark for the performance of turbulence models in the prediction of separated flows (c.f., Abbott and Kline 1962; Briggs, Mellor and Yamada 1977; Kim, Kline and Johnston 1980; Eaton and Johnston 1981; Sindir 1982; Celenligil and Mellor 1985; and Chen 1985). The nonlinear  $K-\epsilon$  model will be shown to yield improved predictions for the reattachment point and turbulence intensities. Comparisons between the computed turbulence statistics and existing experimental data (along with the predictions of other turbulence models) will be made. In addition, the sensitivity of the results to the new empirical constant in the nonlinear model will be examined along with the effect of the Oldroyd derivative terms. The numerical results obtained will be discussed in detail along with other prospective future research.

## 2. THE PHYSICAL PROBLEM

The problem to be considered in this study consists of the turbulent flow of an incompressible viscous fluid past a backward facing step (see Figure 1). The governing equations to be solved are the Reynolds equation and the continuity equation which are of the general form (c.f., Hinze 1975)

$$\rho \left( \frac{\partial \bar{\underline{v}}}{\partial t} + \bar{\underline{v}} \cdot \nabla \bar{\underline{v}} \right) = - \nabla \bar{p} + \mu \nabla^2 \bar{\underline{v}} + \nabla \cdot \underline{\tau} \quad (1)$$

$$\nabla \cdot \bar{\underline{v}} = 0 \quad (2)$$

where

$\bar{\underline{v}}$   $\equiv$  Mean velocity field

$\bar{p}$   $\equiv$  Mean pressure field

$\rho$   $\equiv$  Density of the fluid

$\mu$   $\equiv$  Dynamic viscosity of the fluid

and  $\underline{\tau}$  is the Reynolds stress tensor whose components are given by

$$\tau_{ij} = -\overline{\rho u_i u_j} \quad (3)$$

where  $u$  is the fluctuating part of the velocity field.

In order to achieve closure, equations relating the Reynolds stress tensor to the global history of the mean velocity field are needed. For the linear K- $\epsilon$  model of turbulence, the Reynolds stress tensor is assumed to be of the form (see Hanjalic and Launder 1972)

$$\tau_{ij} = -\frac{2}{3} \rho K \delta_{ij} + 2\rho C_{\mu} \frac{K^2}{\epsilon} \bar{D}_{ij} \quad (4)$$

where

$$K = -\frac{1}{2\rho} \tau_{ii} \quad (5)$$

$$\bar{D}_{ij} = \frac{1}{2} \left( \frac{\partial \bar{v}_i}{\partial x_j} + \frac{\partial \bar{v}_j}{\partial x_i} \right) \quad (6)$$

are, respectively, the turbulent kinetic energy per unit mass, and the mean rate of strain tensor. Here,  $\epsilon$  is the dissipation rate of turbulence, and  $C_{\mu}$  is a dimensionless constant which assumes an approximate value of 0.09.

Typically, at high Reynolds numbers, the turbulent kinetic energy and dissipation rate are modeled by transport equations (c.f., Hanjalic and Launder 1972) of the form

$$\frac{DK}{Dt} = \frac{1}{\rho} \tau_{ij} \frac{\partial \bar{v}_i}{\partial x_j} + C_1 \frac{\partial}{\partial x_i} \left[ \frac{K}{\rho^2 \epsilon} \left( \tau_{jm} \frac{\partial \tau_{ij}}{\partial x_m} - \rho \tau_{ij} \frac{\partial K}{\partial x_j} \right) \right] - \epsilon \quad (7)$$

$$\frac{D\epsilon}{Dt} = -\frac{C_2}{\rho} \frac{\partial}{\partial x_i} \left( \frac{K}{\epsilon} \tau_{ij} \frac{\partial \epsilon}{\partial x_j} \right) + C_3 \frac{\epsilon}{\rho K} \tau_{ij} \frac{\partial \bar{v}_i}{\partial x_j} - C_4 \frac{\epsilon^2}{K} \quad (8)$$

where  $C_1$ ,  $C_2$ ,  $C_3$ , and  $C_4$  are dimensionless constants which take the approximate values of 0.11, 0.15, 1.43, and 1.92, respectively.

The above set of equations are closed, and form the basis for the linear K- $\epsilon$  model. Because of its simple structure, the K- $\epsilon$  model can

be easily incorporated into any Navier-Stokes computer code which allows for a variable viscosity. This feature, together with its accurate predictions of thin turbulent shear flows (i.e., unseparated turbulent boundary layers), has made the model very popular with engineers and scientists (see Rodi 1982). Nevertheless, despite these advantages, the K- $\epsilon$  model is known to yield highly inaccurate predictions for the normal Reynolds stresses. For example, in a fully developed turbulent channel flow (see Figure 2), the linear K- $\epsilon$  model predicts that the normal Reynolds stresses are all equal, i.e., that

$$\tau_{xx} = \tau_{yy} = \tau_{zz} \quad (9)$$

which is in substantial contradiction of experimental data. To be more specific, the experimental data of Laufer (1951) for turbulent channel flow at a Reynolds number of 30,800 indicates that contrary to (9),

$$\frac{||\tau_{yy} - \tau_{xx}||}{||\tau_{xx}||} \approx 0.5, \quad \frac{||\tau_{yy} - \tau_{xx}||}{||\tau_{xy}||} \approx 2.5 \quad (10)$$

where  $||\cdot||$  denotes the maximum norm.

Such serious errors in the normal Reynolds stress difference ( $\tau_{yy} - \tau_{xx}$ ) can yield significant inaccuracies in the calculation of a two-dimensional recirculating flow with the mean velocity

$$\bar{\mathbf{v}} = \bar{u}(x,y)\mathbf{i} + \bar{v}(x,y)\mathbf{j} \quad (11)$$

A problem arises since such a flow is a solution of the vorticity transport equation (which determines the mean velocity)

$$\bar{u} \frac{\partial \bar{\omega}}{\partial x} + \bar{v} \frac{\partial \bar{\omega}}{\partial y} = \nu \nabla^2 \bar{\omega} + \frac{\partial^2 (\tau_{yy} - \tau_{xx})}{\partial x \partial y} + \frac{\partial^2 \tau_{xy}}{\partial x^2} - \frac{\partial^2 \tau_{xy}}{\partial y^2} \quad (12)$$

where  $\nu \equiv \mu/\rho$  is the kinematic viscosity and

$$\bar{\omega} \equiv \frac{\partial \bar{v}}{\partial x} - \frac{\partial \bar{u}}{\partial y}$$

is the mean vorticity. In the recirculation zone of turbulent flow past a backward facing step (see Figure 1), the term

$$\frac{\partial^2 (\tau_{yy} - \tau_{xx})}{\partial x \partial y} \quad (13)$$

(which vanishes in a unidirectional mean turbulent flow or in an unseparated turbulent boundary layer) is of a comparable order of magnitude to the Reynolds shear stress terms on the right-hand-side of (12). This arises from the fact that x-derivatives are of a comparable order of magnitude to the y-derivatives and, as indicated above,  $||\tau_{yy} - \tau_{xx}|| > ||\tau_{xy}||$  in the recirculating zone. Hence, the serious inaccuracies that arise from the linear K- $\epsilon$  model in the calculation of the reattachment point for the backward facing step problem may be largely due to this modeling deficiency in the normal Reynolds stresses (see Speziale 1987).

The linear K- $\epsilon$  model substantially underpredicts the reattachment point for turbulent flow past a backward facing step as discussed extensively at the 1980-81 AFOSR-HTTM Stanford Conference on Turbulence (the separation length  $L/\Delta H$  predicted by this model varies

from 5.2 to 5.5, whereas experiments indicate that it should be approximately 7.0). As alluded to above, a significant cause of this problem may arise from the inability of the linear K- $\epsilon$  model to predict normal Reynolds stress differences accurately. Recently, Speziale (1987) derived a nonlinear generalization of the K- $\epsilon$  model which takes the form

$$\begin{aligned} \tau_{ij} = & -\frac{2}{3} \rho K \delta_{ij} + 2\rho C_{\mu} \frac{K^2}{\epsilon} \bar{D}_{ij} \\ & + 4 C_D C_{\mu}^2 \rho \frac{K^3}{\epsilon^2} (\bar{D}_{im} \bar{D}_{mj} - \frac{1}{3} \bar{D}_{mn} \bar{D}_{mn} \delta_{ij}) \\ & + 4 C_E C_{\mu}^2 \rho \frac{K^3}{\epsilon^2} (\overset{\circ}{\bar{D}}_{ij} - \frac{1}{3} \overset{\circ}{\bar{D}}_{mm} \delta_{ij}) \end{aligned} \quad (14)$$

where

$$\begin{aligned} \bar{D}_{ij} = & \frac{1}{2} \left( \frac{\partial \bar{v}_i}{\partial x_j} + \frac{\partial \bar{v}_j}{\partial x_i} \right) \\ \overset{\circ}{\bar{D}}_{ij} = & \frac{\partial \bar{D}_{ij}}{\partial t} + \bar{v}_k \cdot \bar{v}_k \bar{D}_{ij} - \frac{\partial \bar{v}_i}{\partial x_m} \bar{D}_{mj} - \frac{\partial \bar{v}_j}{\partial x_m} \bar{D}_{mi} \end{aligned} \quad (15)$$

and  $C_D = C_E = 1.68$ . As a result of the presence of the Oldroyd derivative term  $\overset{\circ}{\bar{D}}_{ij}$  and the quadratic terms in  $\bar{D}_{ij}$ , this nonlinear K- $\epsilon$  model is able to describe turbulent memory effects (it bears a certain resemblance to the Rivlin-Ericksen fluids of viscoelastic

flow; see Rivlin 1957) and yields much more accurate predictions for the normal Reynolds stresses in turbulent channel flow.

The Reynolds equation (1) for turbulent flow past a backward facing step has two components which take the form

$$\rho \left( \bar{u} \frac{\partial \bar{u}}{\partial x} + \bar{v} \frac{\partial \bar{u}}{\partial y} \right) = - \frac{\partial \bar{p}}{\partial x} + \frac{\partial \tau_{xx}}{\partial x} + \frac{\partial \tau_{xy}}{\partial y} \quad (16)$$

$$\rho \left( \bar{u} \frac{\partial \bar{v}}{\partial x} + \bar{v} \frac{\partial \bar{v}}{\partial y} \right) = - \frac{\partial \bar{p}}{\partial y} + \frac{\partial \tau_{xy}}{\partial x} + \frac{\partial \tau_{yy}}{\partial y} \quad (17)$$

where (for the nonlinear K- $\epsilon$  model)

$$\begin{aligned} \tau_{xx} = & - \frac{2}{3} \rho K + 2\rho C_{\mu} \frac{K^2}{\epsilon} \frac{\partial \bar{u}}{\partial x} \\ & + \frac{4}{3} \rho C_{\mu}^2 \frac{K^3}{\epsilon^2} \left[ (C_D - 2C_E) \left( \frac{\partial \bar{u}}{\partial x} \right)^2 + \left( \frac{1}{4} C_D - 2C_E \right) \left( \frac{\partial \bar{u}}{\partial y} \right)^2 \right. \\ & \left. + \left( \frac{1}{2} C_D - C_E \right) \left( \frac{\partial \bar{u}}{\partial y} \frac{\partial \bar{v}}{\partial x} \right) + \left( \frac{1}{4} C_D + C_E \right) \left( \frac{\partial \bar{v}}{\partial x} \right)^2 \right] \\ & + 4\rho C_E C_{\mu}^2 \frac{K^3}{\epsilon^2} \left( \bar{u} \frac{\partial^2 \bar{u}}{\partial x^2} - \bar{v} \frac{\partial^2 \bar{v}}{\partial y^2} \right) \end{aligned} \quad (18)$$

$$\begin{aligned} \tau_{yy} = & - \frac{2}{3} \rho K + 2\rho C_{\mu} \frac{K^2}{\epsilon} \frac{\partial \bar{v}}{\partial y} \\ & + \frac{4}{3} \rho C_{\mu}^2 \frac{K^3}{\epsilon^2} \left[ (C_D - 2C_E) \left( \frac{\partial \bar{v}}{\partial y} \right)^2 + \left( \frac{1}{4} C_D - 2C_E \right) \left( \frac{\partial \bar{v}}{\partial x} \right)^2 \right. \end{aligned}$$

$$\begin{aligned}
& + \left( \frac{1}{2} C_D - C_E \right) \left( \frac{\partial \bar{u}}{\partial y} \frac{\partial \bar{v}}{\partial x} \right) + \left( \frac{1}{4} C_D + C_E \right) \left( \frac{\partial \bar{u}}{\partial y} \right)^2 \Big] \\
& + 4\rho C_E C_\mu^2 \frac{K^3}{\epsilon^2} \left( \bar{v} \frac{\partial^2 \bar{v}}{\partial y^2} - \bar{u} \frac{\partial^2 \bar{u}}{\partial x^2} \right) \tag{19}
\end{aligned}$$

$$\begin{aligned}
\tau_{xy} &= \rho C_\mu \frac{K^2}{\epsilon} \left( \frac{\partial \bar{u}}{\partial y} + \frac{\partial \bar{v}}{\partial x} \right) \\
& - 4\rho C_E C_\mu^2 \frac{K^3}{\epsilon^2} \left( \frac{\partial \bar{u}}{\partial y} \frac{\partial \bar{v}}{\partial y} + \frac{\partial \bar{u}}{\partial x} \frac{\partial \bar{v}}{\partial x} \right) \\
& + 2\rho C_E C_\mu^2 \frac{K^3}{\epsilon^2} \left[ \bar{u} \left( \frac{\partial^2 \bar{v}}{\partial x^2} - \frac{\partial^2 \bar{v}}{\partial y^2} \right) + \bar{v} \left( \frac{\partial^2 \bar{u}}{\partial y^2} - \frac{\partial^2 \bar{u}}{\partial x^2} \right) \right] \tag{20}
\end{aligned}$$

$$\tau_{zz} = -\frac{2}{3} \rho K - \frac{4}{3} \rho C_\mu^2 \frac{K^3}{\epsilon^2} (C_D - 2C_E) \left[ \left( \frac{\partial \bar{u}}{\partial x} \right)^2 + \left( \frac{\partial \bar{v}}{\partial y} \right)^2 + \frac{1}{2} \left( \frac{\partial \bar{u}}{\partial y} + \frac{\partial \bar{v}}{\partial x} \right)^2 \right] \tag{21}$$

In deriving (18) - (21), the continuity equation (2) given by

$$\frac{\partial \bar{u}}{\partial x} + \frac{\partial \bar{v}}{\partial y} = 0 \tag{22}$$

has been made use of. Equations (16) - (22) must be supplemented with transport equations for  $K$  and  $\epsilon$ . For the problem under consideration, turbulent diffusive effects can be neglected (see Chen 1985) and, thus, the transport equations (7) - (8) can be simplified to the form

$$\bar{u} \frac{\partial K}{\partial x} + \bar{v} \frac{\partial K}{\partial y} = \frac{1}{\rho} \left[ \tau_{xx} \frac{\partial \bar{u}}{\partial x} + \tau_{xy} \left( \frac{\partial \bar{u}}{\partial y} + \frac{\partial \bar{v}}{\partial x} \right) + \tau_{yy} \frac{\partial \bar{v}}{\partial y} \right] - \epsilon \quad (23)$$

$$\bar{u} \frac{\partial \epsilon}{\partial x} + \bar{v} \frac{\partial \epsilon}{\partial y} = C_3 \frac{\epsilon}{\rho K} \left[ \tau_{xx} \frac{\partial \bar{u}}{\partial x} + \tau_{xy} \left( \frac{\partial \bar{u}}{\partial y} + \frac{\partial \bar{v}}{\partial x} \right) + \tau_{yy} \frac{\partial \bar{v}}{\partial y} \right] - C_4 \frac{\epsilon^2}{K} \quad (24)$$

Equations (16) - (24) represent a closed system of equations for the determination of the mean turbulent flow fields. Of course, these equations must be solved subject to the appropriate boundary conditions. For turbulent flow past a backward facing step, these boundary conditions consist of fully-developed turbulent channel flow sufficiently far upstream and downstream of the step. The law of the wall is applied at the solid boundaries (c.f., Rodi 1982). More details concerning the boundary conditions will be presented in the next section where the numerical approach will be discussed.

### 3. NUMERICAL METHOD

In this study, the Imperial College's TEACH (Teaching Elliptic Axisymmetry Characteristics Heuristically) computer program will be used since it was written for the calculation of recirculating flows and performs reasonably well for such problems (see Lilley and Rhode 1982). Furthermore, because this program is based on the linear  $K-\epsilon$  model, it is a relatively straightforward process to incorporate the nonlinear  $K-\epsilon$  model (this simply requires the addition of the appropriate nonlinear terms where the Reynolds stresses appear).

The TEACH computer program will be implemented on the nonuniform finite difference mesh shown in Fig. 3. This  $166 \times 73$  finite difference mesh spans 5 step heights upstream and 30 step heights downstream from the step. The grids are uniform and extremely dense in the recirculation region and in the vicinity of step corners in order to conveniently calculate and adequately resolve the higher-order velocity gradients. Special merits of the staggered grid system used in the TEACH code are discussed in Gosman and Pun 1974, and Gosman and Ideriah 1976. The scheme is second-order accurate overall since the first-order derivatives are evaluated by central differences over a single mesh spacing (c.f., Roache 1972). However, in evaluating second-order derivatives (which are needed in the nonlinear model), this nonuniform mesh requires a more complex finite difference expression which has a second-order accurate form given by

$$f''(i) = 2 \left[ \frac{f(i+1) \Delta_-^3 - f(i)(\Delta_-^3 + \Delta_+^3) + f(i-1) \Delta_+^3}{\Delta_+^2 \Delta_-^2 (\Delta_+ + \Delta_-)} + f'(i) \left( \frac{\Delta_+ - \Delta_-}{\Delta_+ \Delta_-} \right) \right] \quad (25)$$

where  $f(i)$  is any function,  $f'(i)$  is its first derivative,  $f''(i)$  is its second derivative,  $\Delta_+$  is the mesh spacing in the forward direction, and  $\Delta_-$  is the mesh spacing in the backward direction. Equation (25) can be applied for the calculation of second partial derivatives with respect to  $x$  or  $y$  (by invoking the continuity equation, no mixed derivatives in  $x$  and  $y$  need to be calculated). Since this finite-difference expression requires the value for  $f'$ , which is not exact, this expression is actually somewhat less than second-order accurate. Hence, the application of equation (25) is limited to outside of the recirculation zone where second derivative contributions are small. Within, and immediately adjacent to, the recirculation zone (where the mesh is uniform), fourth-order accurate expressions for the first and second derivative terms in the Reynolds stresses are used that are given by

$$f'(i) = \frac{-f(i+2) + 8f(i+1) - 8f(i-1) + f(i-2)}{12\Delta} \quad (26)$$

$$f''(i) = \frac{-f(i+2) + 16f(i+1) - 30f(i) + 16f(i-1) - f(i-2)}{12\Delta^2} \quad (27)$$

A top hat filtering scheme is used to smooth any numerical fluctuations which arise due to the steep velocity gradients. The reader is referred to Isaacson and Keller (1966) for more details on these numerical representations.

In the TEACH code, the governing equations for the linear K- $\epsilon$  model are the continuity equation, the x and y components of the Reynolds equation, and the kinetic energy and dissipation rate transport equations as given in the previous section. The Poisson equation for pressure (obtained by taking the divergence of the Reynolds equation (1)) is also used since the solution procedure here is based on primitive variables (i.e., is based on pressure-velocity as opposed to the stream function-vorticity approach). Since the problem considered is at very high Reynolds numbers (above 100,000), the contributions of the diffusion terms in the transport equations for K and  $\epsilon$  are quite small and can be neglected. For more details on this general numerical method, the reader is referred to Lilley and Rhode (1982).

The governing equations for the nonlinear K- $\epsilon$  model are the same as for the linear model except for the differences in the expressions for the Reynolds stresses. Since the additional nonlinear terms in the Reynolds stresses are not extremely large, they are simply treated as added source terms in the TEACH code. It should be noted that the variables

$$\bar{u}, \bar{v}, \frac{\partial \bar{u}}{\partial x}, \frac{\partial \bar{u}}{\partial y}, \frac{\partial \bar{v}}{\partial x}, \frac{\partial \bar{v}}{\partial y}, K, \epsilon$$

are already calculated for the linear K- $\epsilon$  model and, hence, are generated by the basic TEACH code. The only new variables that need to be calculated are the second derivatives of the velocity fields

$$\frac{\partial^2 \bar{u}}{\partial x^2}, \frac{\partial^2 \bar{u}}{\partial y^2}, \frac{\partial^2 \bar{v}}{\partial x^2}, \frac{\partial^2 \bar{v}}{\partial y^2}.$$

Inside the recirculation region, these second derivatives are computed by the fourth-order accurate finite difference scheme given by equation (27). A lower-order accurate scheme was tried, but it yielded some fluctuations in these derivative fields (especially within the recirculation zone) due to its inability to resolve the steep velocity gradients. This problem persisted (although to a substantially lesser extent) even with the higher-order accurate scheme and therefore a smoothing filter was employed. As alluded to earlier, a top hat filter was used. This filter can be applied to a field more than one time, yielding a smoother result after each pass. The velocity fields are filtered once before they are used in evaluating first and second derivatives. As mentioned before, a fourth-order accurate expression is also used to calculate the first derivatives within the recirculation zone in the nonlinear Reynolds stress calculations. It should be noted that at the solid boundaries, an outward Taylor expansion is used to evaluate the derivatives.

After obtaining the first and second order derivatives, the nonlinear part of each Reynolds stress is readily obtained from equations (18) - (21). In order to incorporate these nonlinear Reynolds stress terms into the program, the linear representations for the Reynolds stresses were located in the various parts of the TEACH code, and the nonlinear terms were added in an appropriate fashion.

Computations were conducted in a channel with an expansion ratio of 3:2 at a Reynolds number of approximately 132,000 (based on the upstream centerline mean velocity and downstream channel width). The program was run with an automatic vectorizer on the CYBER 205 computer at the University of Georgia. Iterations were performed until a converged solution was obtained based on a residual source criterion (see Lilley and Rhode 1982). Approximately 90 minutes of CPU time were required on a 166x73 mesh for the nonlinear K- $\epsilon$  model to converge, whereas only about 45 minutes were needed for the linear K- $\epsilon$  model. The number of steps required for a converged solution depends on the model and the input conditions and varied from 400 to 1000 iterations. The closer that the initial guess of the variable fields is to the actual solution, the less iterations are needed. However, by a comparison of the rate that the residual sources decrease, it was clear that the nonlinear model converges at a slower rate than the linear model. This is not very surprising considering the fact that the nonlinear K- $\epsilon$  model contains Reynolds stress relaxation terms which are dispersive rather than dissipative. The detailed numerical results obtained will be discussed in the next section.

#### 4. DISCUSSION OF THE RESULTS

We will now present the computed results obtained for turbulent flow over a backward facing step for a Reynolds number  $Re = 132,000$  and an expansion ratio of 3:2. The computed streamlines and mean velocity profiles obtained from the linear  $K-\epsilon$  model are shown in Fig. 4 which clearly indicate a reattachment length of  $L/\Delta H = 5.5$  -- a value in the range of previously conducted computations. This compares rather unfavorably to the experimental value of  $L/\Delta H = 7.0$  (see Kim, Kline, and Johnston 1980). The nondimensional turbulence intensity  $(\overline{uu})^{1/2}$  and shear stress  $\overline{uv}$  obtained from the linear  $K-\epsilon$  model are shown in Figs. 5-6 alongside the available experimental data (reliable experimental data is not available for the recirculation zone). The computed streamlines and mean velocity profiles obtained from the nonlinear  $K-\epsilon$  model, shown in Fig. 7, clearly demonstrate an improved prediction for the reattachment point of  $L/\Delta H = 6.4$ . This improvement is probably due to the better prediction of the turbulence intensities in the recirculation zone (the reader should compare Figs. 8-9 with Figs. 5-6). However, since no reliable Reynolds stress data is available inside the recirculation zone (due to flow oscillations), the present conclusion must rest on comparisons of data from Kim, Kline, and Johnston (1980) downstream of the reattachment point.

Comparisons will now be made between the results of the nonlinear  $K-\epsilon$  model and those obtained from second-order closure models. As shown in Fig. 10, the second-order closure model of Briggs, Mellor,

and Yamada (1977) predicts a reattachment length of  $L/\Delta H = 8.0$  (it should be noted, however, that in a more recent study of this model conducted by Celenligil and Mellor 1985, a result  $L/\Delta H = 7.7$  was claimed which is of a comparable accuracy to the result of  $L/\Delta H = 6.4$  predicted by the nonlinear  $K-\epsilon$  model). The reasons for this compatibility are more apparent when Reynolds stress results are compared. As shown in Fig. 11, the turbulence intensity predictions of the nonlinear  $K-\epsilon$  model and the second-order closure model are in good qualitative agreement throughout the unseparated flow. The turbulent shear stress predictions shown in Fig. 12 are not in as good agreement inside the recirculation zone (it is unfortunate that no reliable data is available in this region in order to make a critical comparison). However, in so far as the reattachment point is concerned, it is clear that the nonlinear  $K-\epsilon$  model yields comparably good, if not better, results to second-order closure models with the need for substantially less calculations (second-order closure models require a higher level of computation since transport equations must be solved for each component of the Reynolds stress tensor).

The nonlinear  $K-\epsilon$  model examined herein introduces two new empirical constants,  $C_D$  and  $C_E$ , in equation (14). These constants were found to assume a value of 1.68 by correlating with experimental data for normal Reynolds stress differences in turbulent channel flow (Speziale 1986). However, the accuracy of this data is somewhat questionable; errors of the order of 10% can easily occur. Consequently, calculations were performed to test the sensitivity of

the computed results to the precise value of  $C_D$  and  $C_E$ . For this purpose, the computations were repeated for  $C_D = C_E = 1.40$ . The computed streamlines and turbulence intensity for this case are compared with the previous computations in Figs. 13 - 14. There is no significant difference in the two results, indicating that even a 15% error in the predicted value of  $C_D$  and  $C_E$  would have little effect on the major conclusions of this study.

Computer runs were also made for the nonlinear  $K-\epsilon$  model where the second-order derivative terms of the mean velocity arising from the Oldroyd derivative in (14) are set to zero (such a resulting model bears a qualitative resemblance to previous nonlinear models proposed by Lumley 1970 and Saffman 1977). As shown in Fig. 15, without the second-order derivatives, the resulting reattachment length reduces a significant amount to a value of  $L/\Delta H = 6.0$ . This shortening of  $L/\Delta H$  is not unexpected since the second derivative terms have a dispersive character which would reduce the dissipation in the separated zone allowing it to expand. It is rather surprising, however, that the elimination of the second derivative terms had a relatively small effect on the turbulent stress intensity shown in Fig. 16. Since the second derivative terms generally are of a comparable order of magnitude to the first derivative terms squared (see equations (18) - (21)), one might expect the contribution of these terms to be more significant in the turbulence intensity predictions. Hence considering their substantial impact on the reattachment point, the most dominant contribution of the second derivative terms must be in

the prediction of normal Reynolds stress differences (quantities which play an important role in the calculation of a recirculating flow as discussed earlier). Thus, it is clear that the Oldroyd derivative (which distinguishes this new nonlinear  $K-\epsilon$  model from all previous such nonlinear models) plays a significant role in the turbulent backward facing step calculation.

Unfortunately, as discussed in Section 3, the accurate evaluation of higher-order derivatives is extremely difficult even with a fourth-order accurate finite difference scheme. In this study, a top hat filter was used to alleviate some localized numerical fluctuations in these derivatives. Since the top hat filter is an averaging algorithm, it also somewhat reduces the steep velocity gradients in the flow, thus adding to the problem of numerical accuracy. However, this problem is a localized one and any adverse consequences of filtering appears to be in the direction of underpredicting the reattachment point as a result of smoothing. Some initial computations that were conducted without filtering (which must be viewed with suspicion as a result of fluctuations in the second derivative terms) yielded a reattachment length of  $L/\Delta H = 6.7$ . Thus, it appears that the more accurate calculation of the second derivatives is likely to bring the computed results of this study in closer agreement with experimental observations. It is our opinion, however, that such improvements in the numerical algorithm are unlikely to make more than a 5 or 6% change in the numerical results presented herein.

## 5. CONCLUSIONS

The nonlinear K- $\epsilon$  model examined in this study has been shown to yield considerably improved predictions for the reattachment point for turbulent flow past a backward facing step. To be specific, the nonlinear K- $\epsilon$  model was shown to predict a separation length of  $L/\Delta H = 6.4$  as compared to the experimental value of  $L/\Delta H = 7.0$ . This result constitutes a substantial improvement on the value of  $L/\Delta H$  in the range of 5.2 - 5.5 predicted by the linear K- $\epsilon$  model and is of a comparable accuracy to results obtained from the substantially more complicated second-order closure models (e.g., Celenligil and Mellor 1985 obtained a separation length of  $L/\Delta H = 7.7$ ). From an analysis of the mean vorticity transport equation, it was argued that these improved results probably arise from the nonlinear K- $\epsilon$  model's ability to predict normal Reynolds stress differences more accurately. While there is no reliable experimental data for the Reynolds stresses inside the recirculation zone, the results obtained from the nonlinear K- $\epsilon$  model are in the range of those obtained from second-order closure models and appear to constitute an improvement over those predicted by the linear K- $\epsilon$  model.

Several questions about the accuracy of the numerical results presented in this study still need to be resolved as is true of most numerical studies of the backward facing step problem. The TEACH code has certain undesirable features in its convergence properties when terms (such as the nonlinear contributions to the Reynolds stresses)

which are not purely dissipative are added. Furthermore, as a result of the large velocity gradients in the recirculation region, it was extremely difficult to calculate higher order derivatives of the velocity field in a highly accurate fashion. However, as a direct consequence of the smoothing properties of the top hat filter, it appears that any errors in the computed reattachment point would be in the direction of underprediction, thus, putting the results obtained herein in closer agreement with the experimental data. Nonetheless, it would be useful to check these results using several alternative numerical algorithms. Likewise, it would be of value to consider other geometries. Unfortunately, such investigations are beyond the scope of the present study and must await future research. Although several questions remain to be answered, the results obtained in this study are extremely encouraging and strongly support the pursuit of future investigations of this nonlinear  $K-\epsilon$  model which may prove to be of considerable value in the future analysis of a variety of turbulence problems.

#### **ACKNOWLEDGEMENTS**

The authors would like to thank the Advanced Computational Methods Center of the University of Georgia for the CYBER 205 computer time made available and Dr. C.P. Chen for allowing us the use of his computer program.

**REFERENCES**

- Abbott, D.E. and Kline, S. J. 1962, Experimental Investigation of Subsonic Turbulent Flow Over Single and Double Backward Facing Steps. **ASME Journal of Basic Engineering D84**, 317.
- Batchelor, G.K. 1967, **Introduction to Fluid Dynamics**, Cambridge Univ. Press, London.
- Briggs, M., Mellor, G. and Yamada, T. 1977, A Second Moment Turbulence Model Applied to Fully Separated Flow, in **Project SQUID Workshop on Turbulence in Internal Flows**, S. Murthy, ed., Hemisphere Pub. Corp., 249.
- Celenligil, M.C. and Mellor, G.L. 1985, Numerical Solution of Two-Dimensional Turbulent Separated Flows Using a Reynolds Stress Closure Model. **ASME J. Fluids Engineering 107**, 467.
- Chen, C.P. 1985, Multiple Scale Turbulence Closure Modeling of Confined Recirculating Flows. NASA CR-178536, NASA-Marshall Space Flight Center.
- Eaton, J.K. and Johnston, J.P. 1981, A Review of Research on Subsonic Turbulent Flow Reattachment. **AIAA J. 19**, 1093.
- Gessner, F.B. and Emery, A.F. 1976, A Reynolds Stress Model for Turbulent Corner Flows - Part I: Development of the Model. **ASME J. Fluids Eng. 98**, 261.
- Gosman, A.D. and Pun, W.M. 1974, Calculation of Recirculating Flows. Report no. HTS/74/12, Department of Mechanical Engineering, Imperial College, London.

- Gosman, A.D. and Ideriah, F.J.K. 1976, TEACH-2E: A General Computer Program for Two-Dimensional, Turbulent, Recirculating Flows. Report, Department of Mechanical Engineering, Imperial College, London.
- Hanjalic, K. and Launder, B.E. 1972, A Reynolds Stress Model of Turbulence and its Application to Thin Shear Flows. **J. Fluid Mech.** 52, 609.
- Hinze, J.O. 1975, **Turbulence**, McGraw-Hill.
- Isaacson, E. and Keller H.B. 1966, **Analysis of Numerical Methods**. Wiley.
- Kim, J., Kline, S. J. and Johnston, J.P. 1980, Investigation of a Reattaching Turbulent Shear Layer: Flow Over a Backward-Facing Step. **ASME J. Fluids Eng.** 102, 302.
- Laufer, J. 1951, Investigation of Turbulent Flow in a Two-Dimensional Channel. **NACA TN 1053**.
- Launder, B.E. and Ying, W.M. 1971, Fully Developed Turbulent Flow in Ducts of Square Cross Section. Report TM/TN/A/11, Imperial College of Science and Technology.
- Lilley, D.G. and Rhode, D.L. 1982, A Computer Code for Swirling Turbulent Axisymmetric Recirculating Flows in Practical Isothermal Combustor Geometries, NASA Contractor Report 3442.
- Lumley, J.L. 1970, Toward a Turbulent Constitutive Relation. **J. Fluid Mech.** 41, 413.

- Rivlin, R.S. 1957, The Relation Between the Flow of Non-Newtonian Fluids and Turbulent Newtonian Fluids. **Quart. Appl. Math** 15, 212.
- Roache, P.J. 1972, **Computational Fluid Dynamics**. Hermosa Publishers, Albuquerque.
- Rodi, W. 1982, Examples of Turbulence Models for Incompressible Flows. **AIAA** 20, 872.
- Saffman, P.G. 1977, Results of a Two Equation Model for Turbulent Flow and Development of a Relaxation Stress Model for Application to Straining and Rotating Flows, in **Project SQUID Workshop on Turbulence in Internal Flows**. S. Murthy, ed., Hemisphere Publisher.
- Sindir, M.M.S. 1975, A Numerical Study of Turbulent Flows in Backward-Facing Step Geometries: A Comparison of Four Models of Turbulence. Ph.D. Thesis, University of California, Davis.
- Speziale, C.G. 1987, On Nonlinear K- $\ell$  and K- $\epsilon$  Models of Turbulence. **J. Fluid Mech.** 178.

## LIST OF FIGURES

- Figure 1. Turbulent flow past a backward facing step.
- Figure 2. Fully-developed turbulent channel flow.
- Figure 3. Finite difference mesh (166x73).
- Figure 4. Computed results obtained for the linear K- $\epsilon$  model: (a) streamlines (b) mean velocity profiles.
- Figure 5. Dimensionless turbulence intensities obtained from the linear K- $\epsilon$  model.
- Figure 6. Dimensionless turbulent shear stress obtained from the linear K- $\epsilon$  model.
- Figure 7. Computed results obtained for the nonlinear K- $\epsilon$  model: (a) streamlines (b) mean velocity profiles.
- Figure 8. Dimensionless turbulence intensities obtained from the nonlinear K- $\epsilon$  model.
- Figure 9. Dimensionless turbulent shear stress obtained from the nonlinear K- $\epsilon$  model.
- Figure 10. Comparison of computed streamlines: (a) for the second-order closure model of Briggs, Mellor, and Yamada (1977), and (b) for the nonlinear K- $\epsilon$  model.
- Figure 11. Comparison of turbulence intensities obtained from the second-order closure model of Celenligil and Mellor (1985) and the nonlinear K- $\epsilon$  model.
- Figure 12. Comparison of turbulent shear stresses obtained from the second-order closure model of Celenligil and Mellor (1985) and the nonlinear K- $\epsilon$  model.
- Figure 13. Computed streamlines obtained for the nonlinear K- $\epsilon$  model: (a)  $C_D=C_E=1.40$  (b)  $C_D=C_E=1.68$ .
- Figure 14. Turbulence intensities obtained from the nonlinear K- $\epsilon$  model: (a)  $C_D=C_E=1.40$  and (b)  $C_D=C_E=1.68$ .
- Figure 15. Computed streamlines obtained for the nonlinear K- $\epsilon$  model without the second derivative terms.
- Figure 16. Dimensionless turbulence intensities for the nonlinear K- $\epsilon$  model without the second derivative terms.

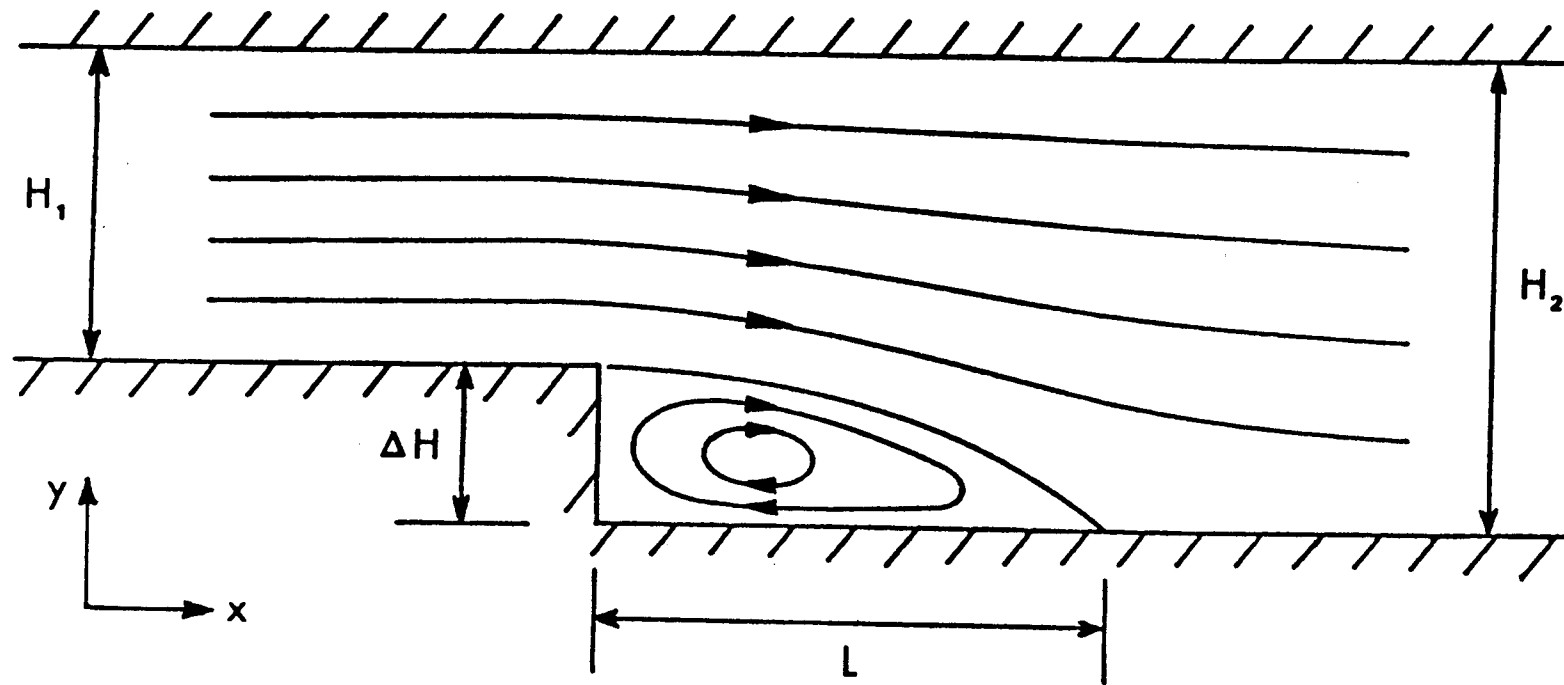


FIGURE 1. Turbulent flow past a backward facing step.

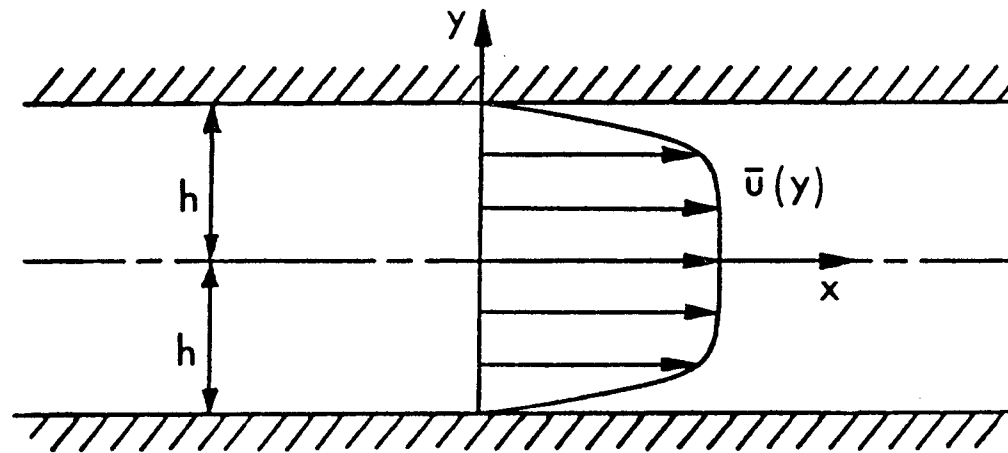
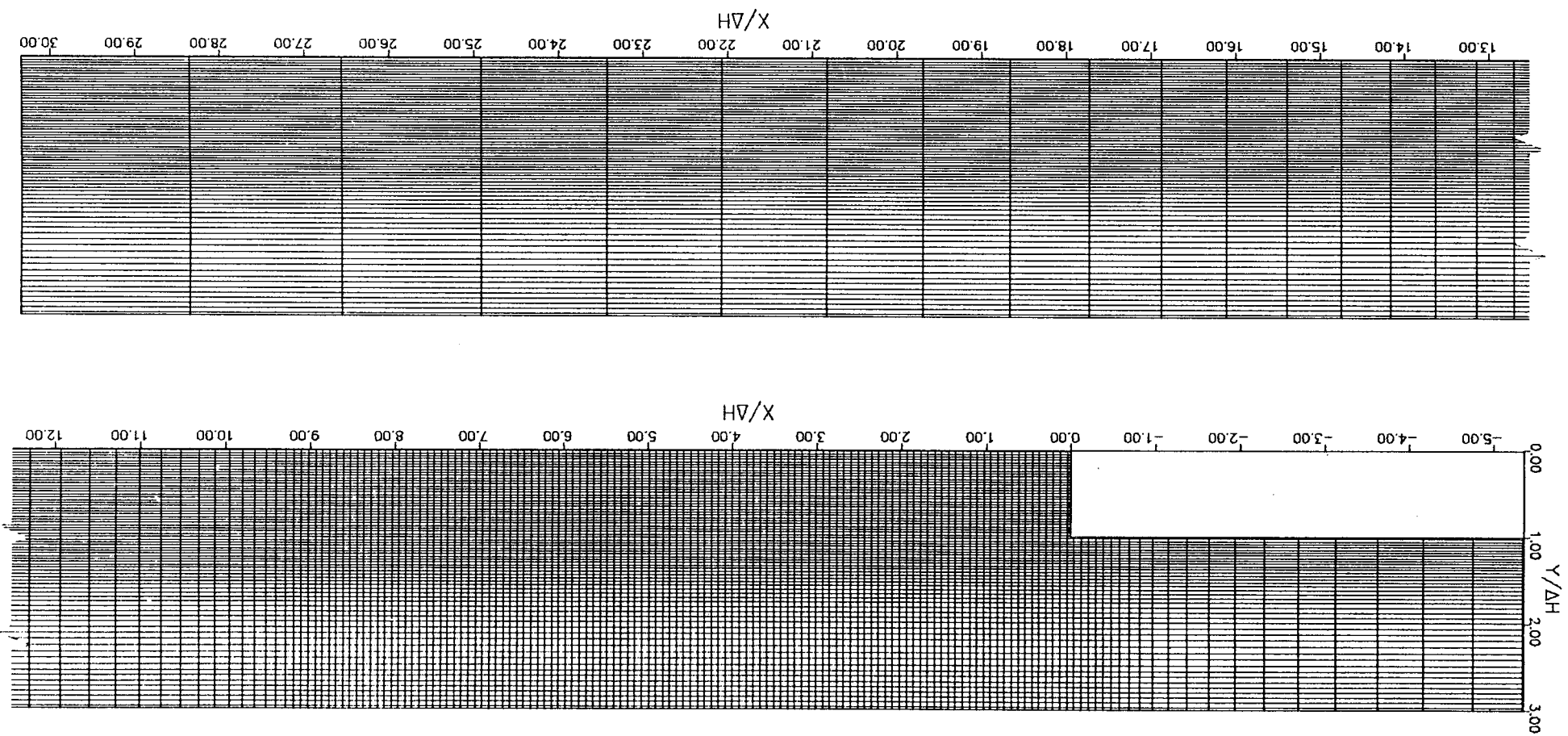
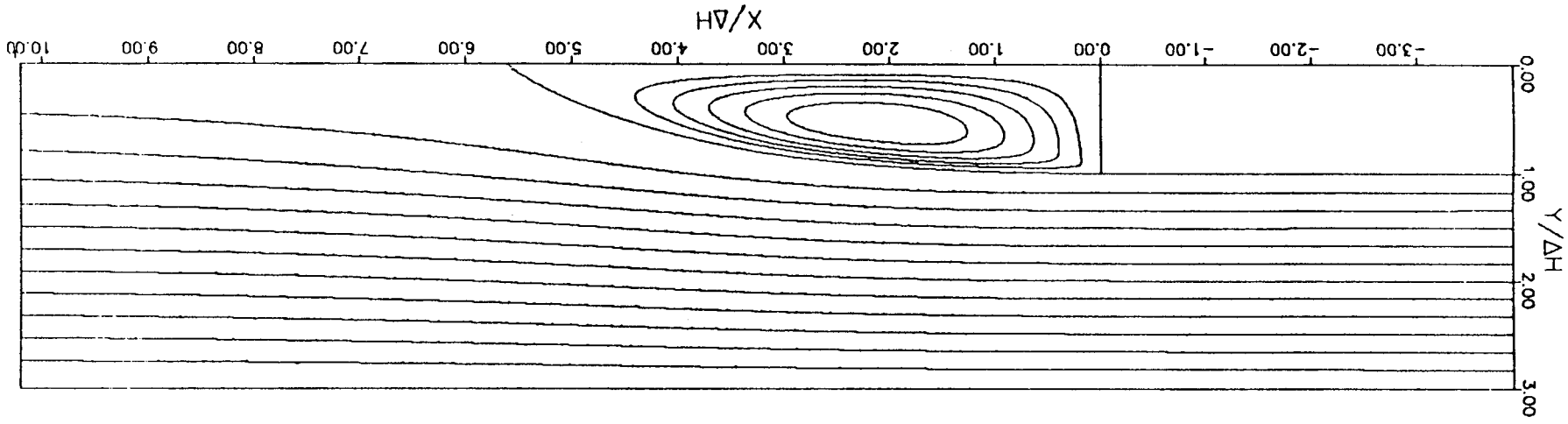


FIGURE 2. Fully-developed turbulent channel flow.

FIGURE 3. Finite difference mesh (166X73).





(a)

FIGURE 4. Computed results obtained for the linear  $k-\epsilon$  model:  
 (a) Streamlines  
 (b) Mean velocity profiles

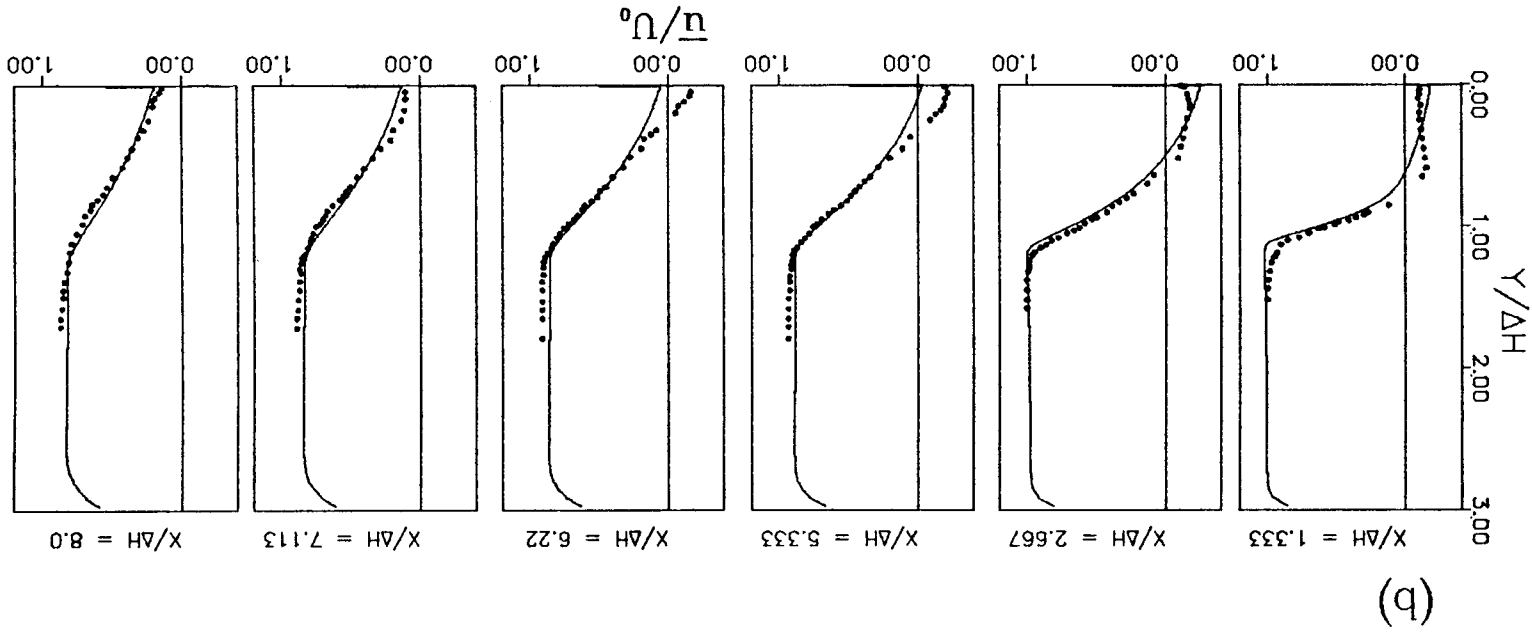


FIGURE 4. Computed results obtained for the linear k- $\epsilon$  model:  
 (a) Streamlines  
 (b) Mean velocity profiles

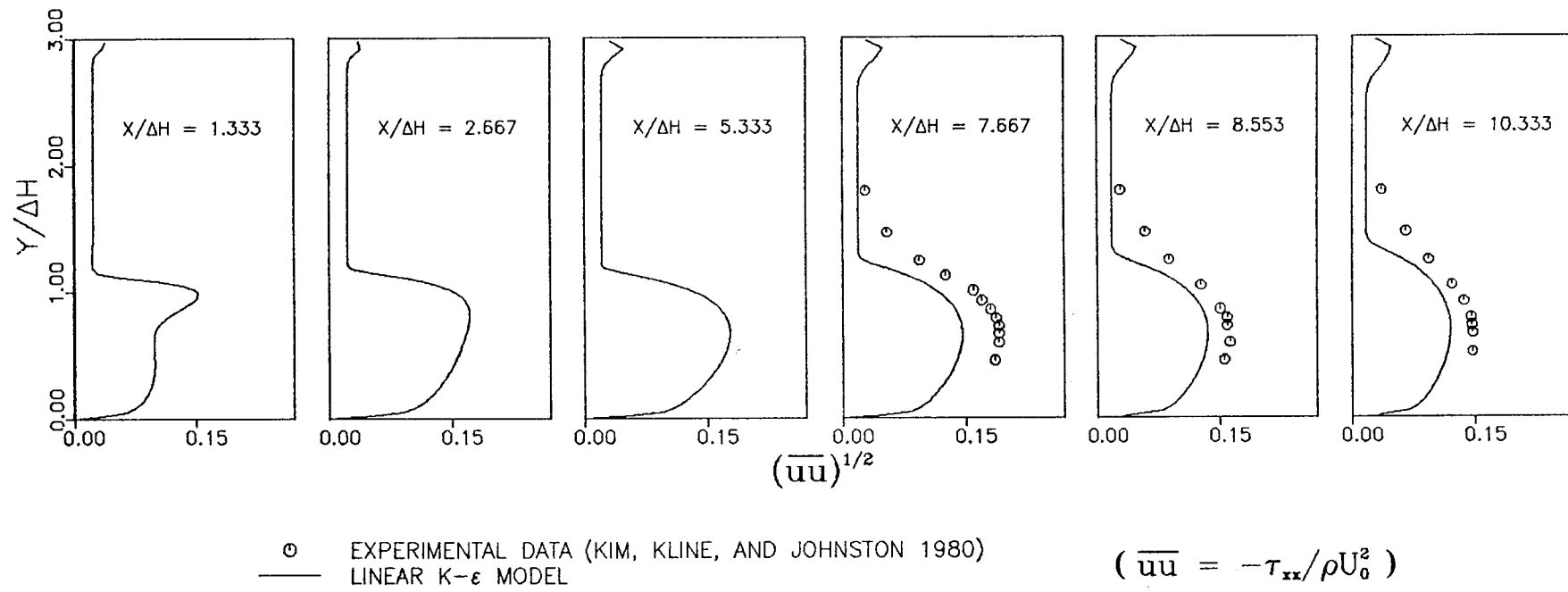
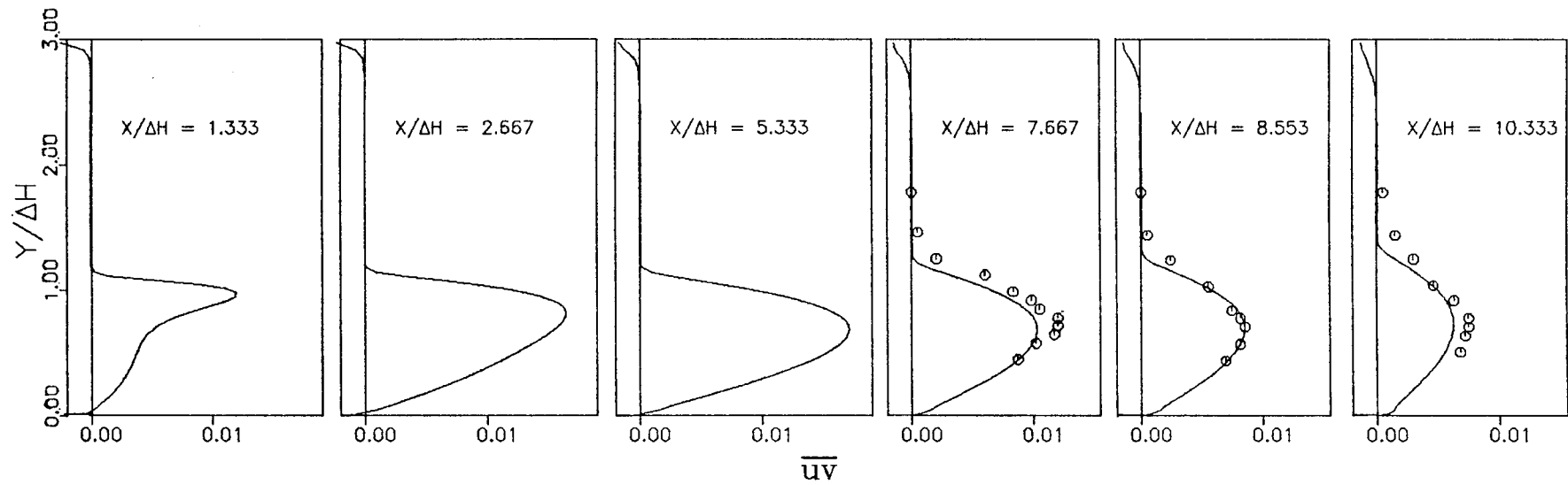


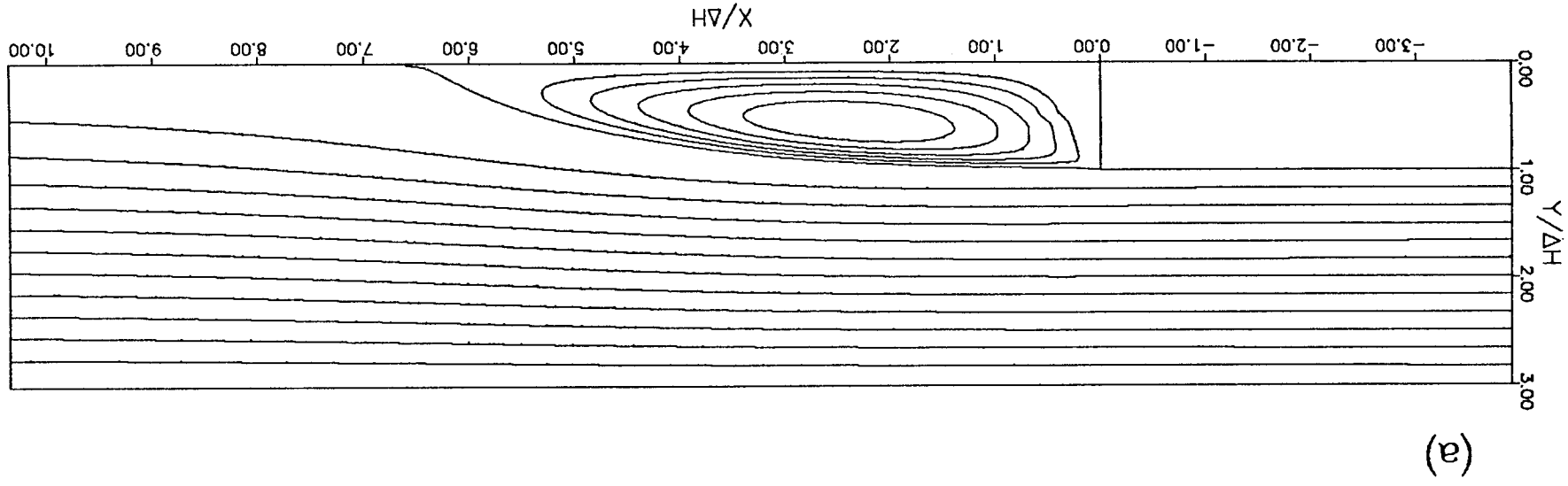
FIGURE 5. Dimensionless turbulence intensities obtained from the linear K- $\epsilon$  model.



○ EXPERIMENTAL DATA (KIM, KLINE, AND JOHNSTON 1980)      (  $\overline{u'v'} = -\tau_{xy}/\rho U_0^2$  )  
 — LINEAR K- $\epsilon$  MODEL

FIGURE 6. Dimensionless turbulent shear stress obtained from the linear K- $\epsilon$  model.

FIGURE 7. Computed results obtained for the nonlinear K- $\epsilon$  model:  
(a) Streamlines  
(b) Mean velocity profiles



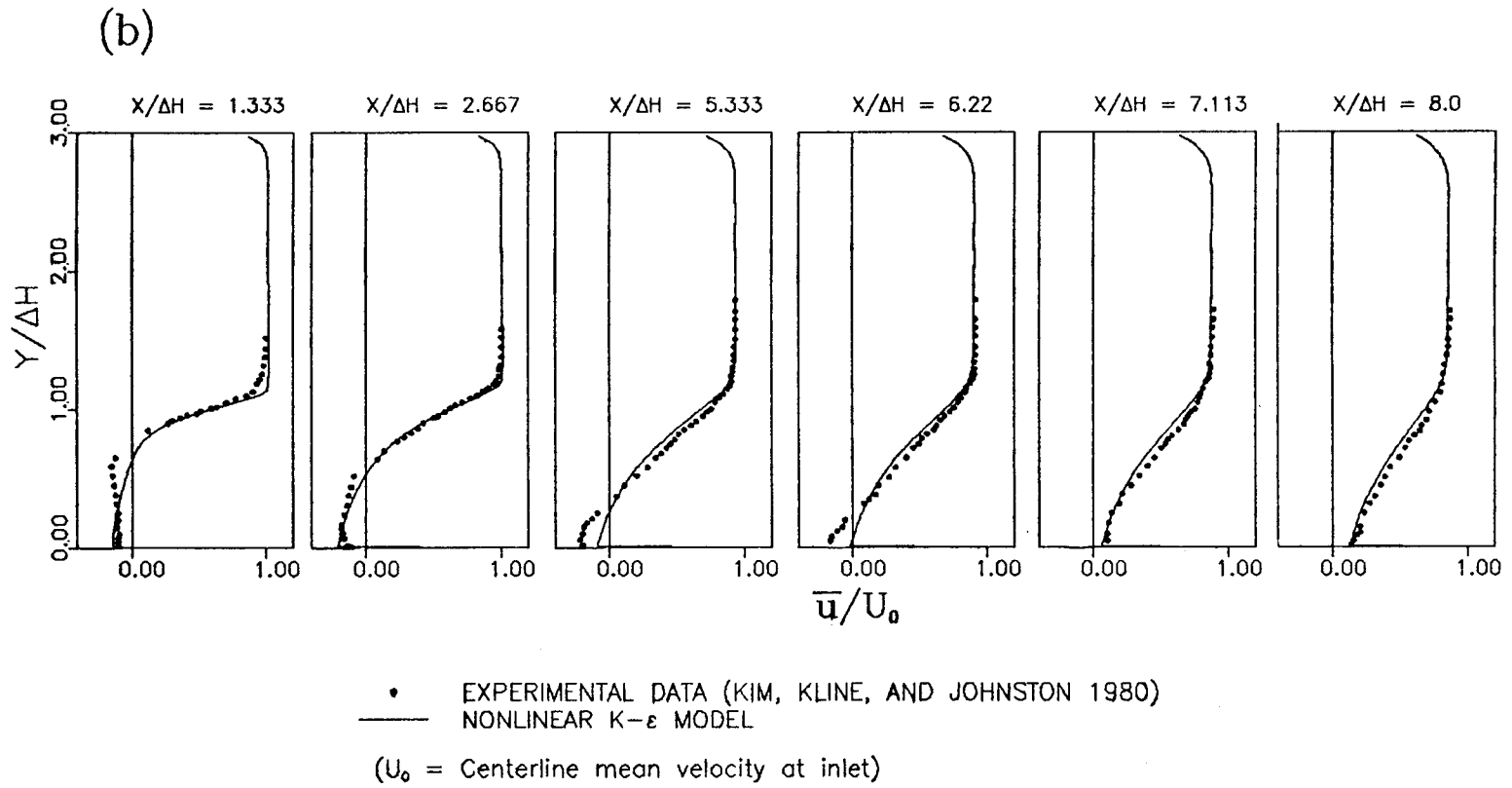


FIGURE 7. Computed results obtained for the nonlinear K- $\epsilon$  model :

(a) Streamlines

(b) Mean velocity profiles

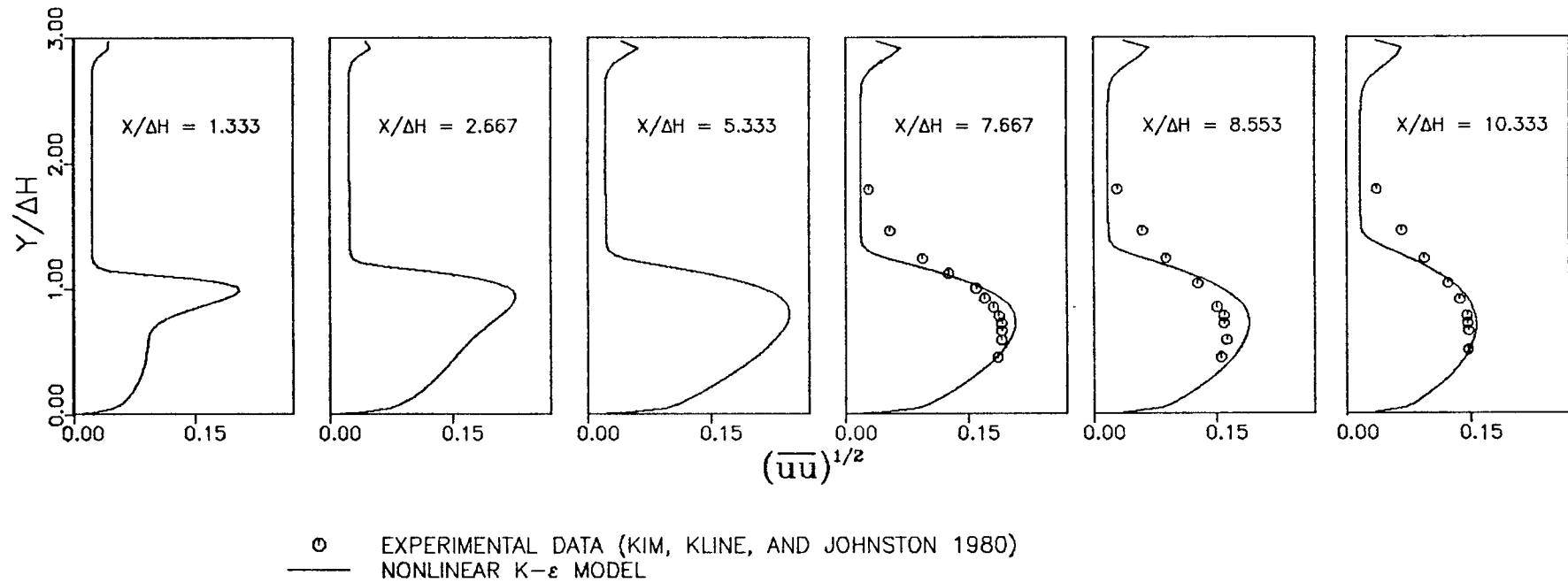


FIGURE 8. Dimensionless turbulence intensities obtained from the nonlinear  $K-\epsilon$  model.

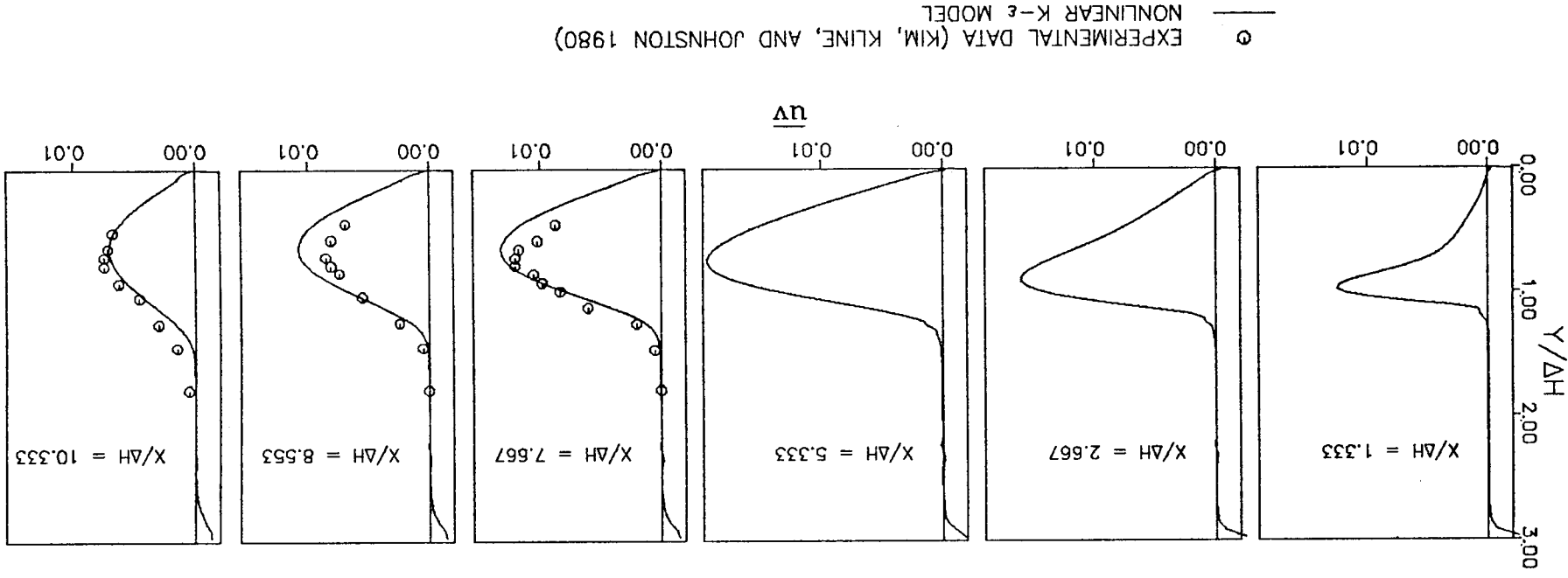
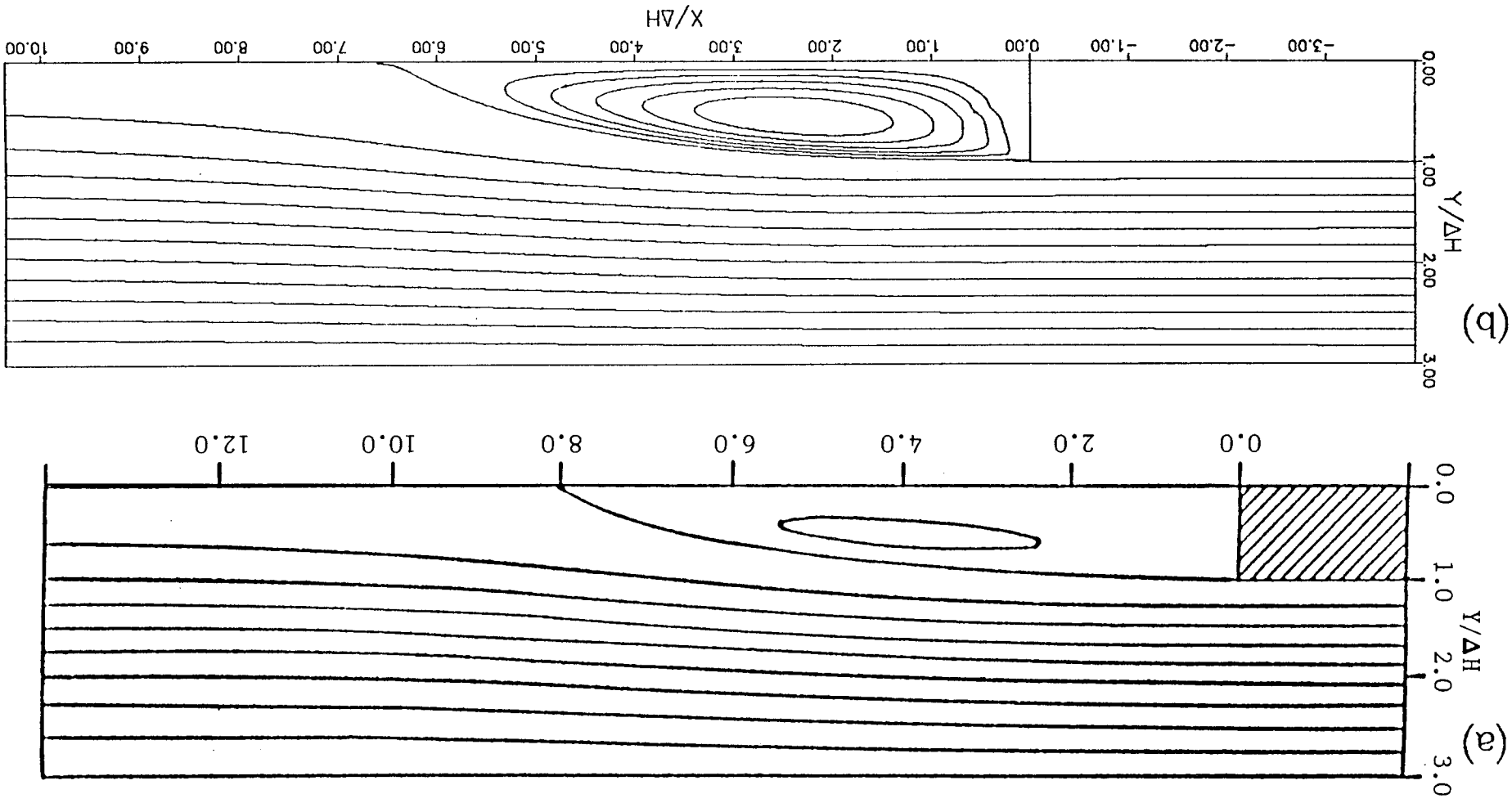
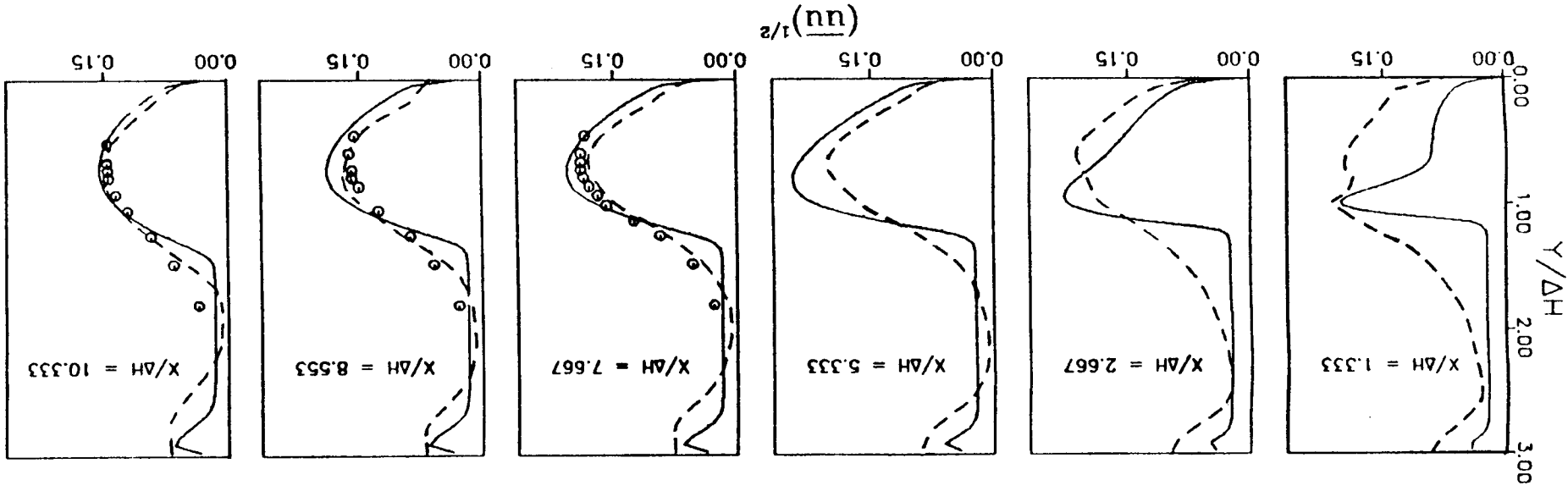


FIGURE 9. Dimensionless turbulent shear stress obtained from the nonlinear  $K-\epsilon$  model.

FIGURE 10. Comparison of computed streamlines: (a) for the second-order closure model of Briggs, Mellor, and Yamada (1977), and (b) for the nonlinear  $k-\epsilon$  model.

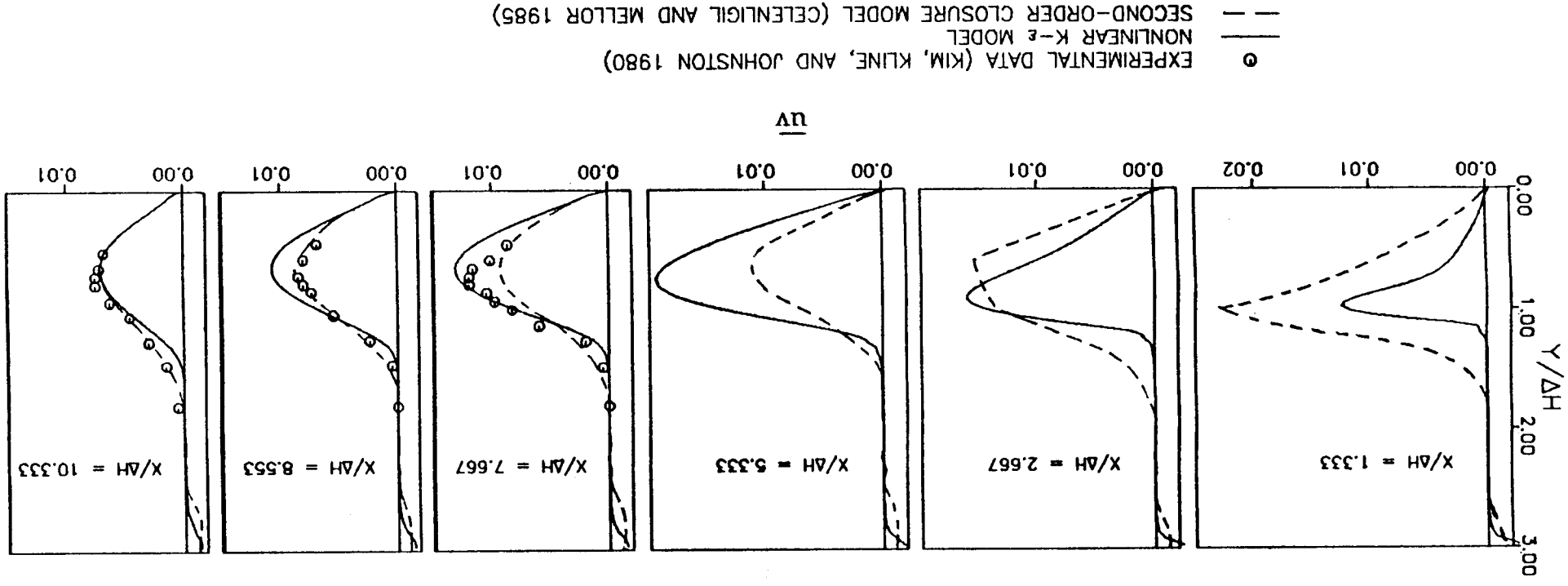




○ EXPERIMENTAL DATA (KIM, KLINE, AND JOHNSTON 1980)  
 ——— NONLINEAR  $K-\epsilon$  MODEL  
 - - - SECOND-ORDER CLOSURE MODEL (CELENLIGIL AND MELLOR 1985)

FIGURE 11. Comparison of turbulence intensities obtained from the second-order closure model of Celenligil and Mellor (1985) and the nonlinear  $K-\epsilon$  model.

FIGURE 12. Comparison of turbulent shear stresses obtained from the second-order closure model of Celenligil and Mellor (1985) and the nonlinear  $k-\epsilon$  model.



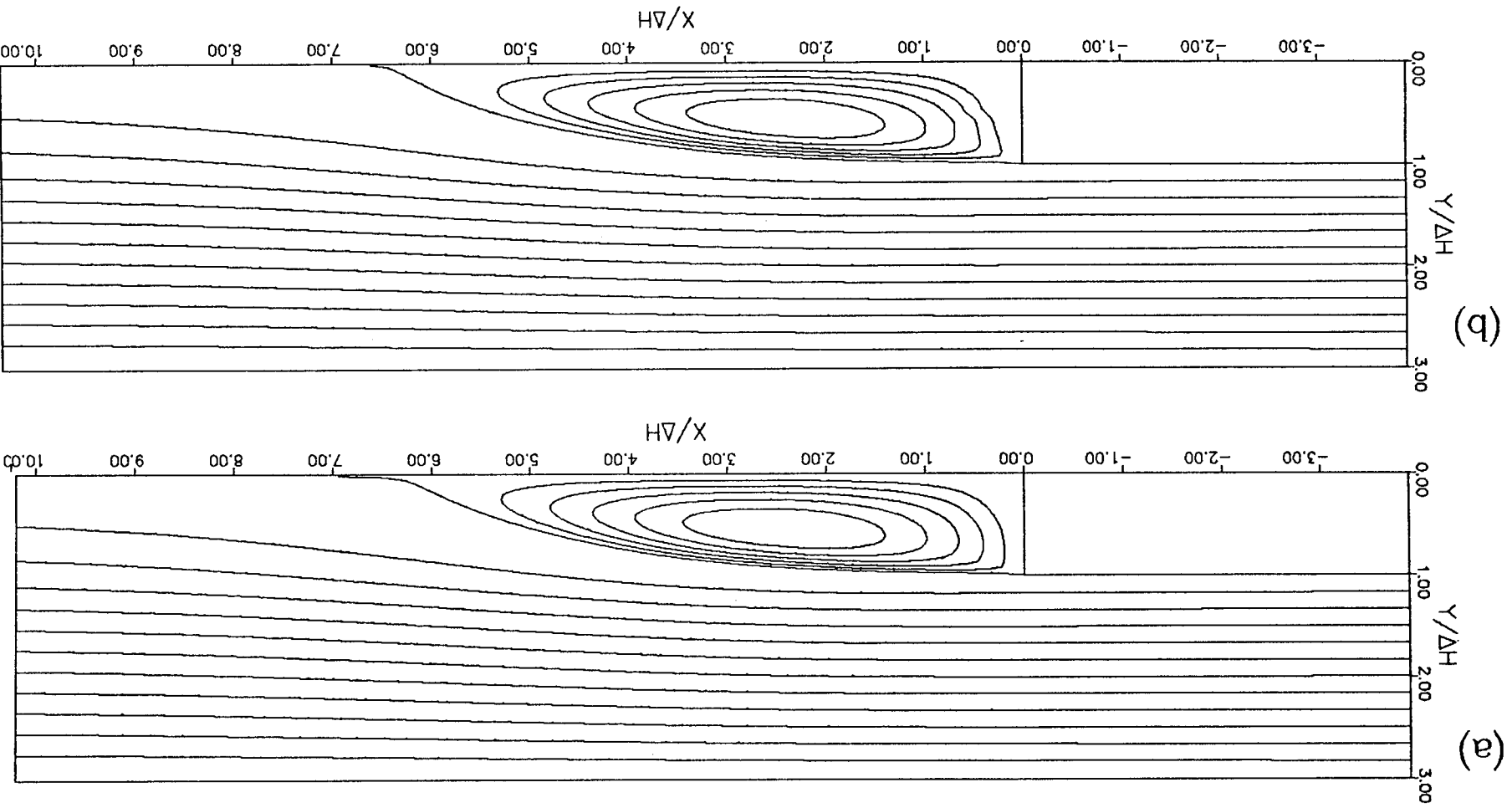


FIGURE 13. Computed streamlines obtained for the nonlinear K- $\epsilon$  model: (a)  $C_p = C_e = 1.40$  and (b)  $C_p = C_e = 1.68$ .

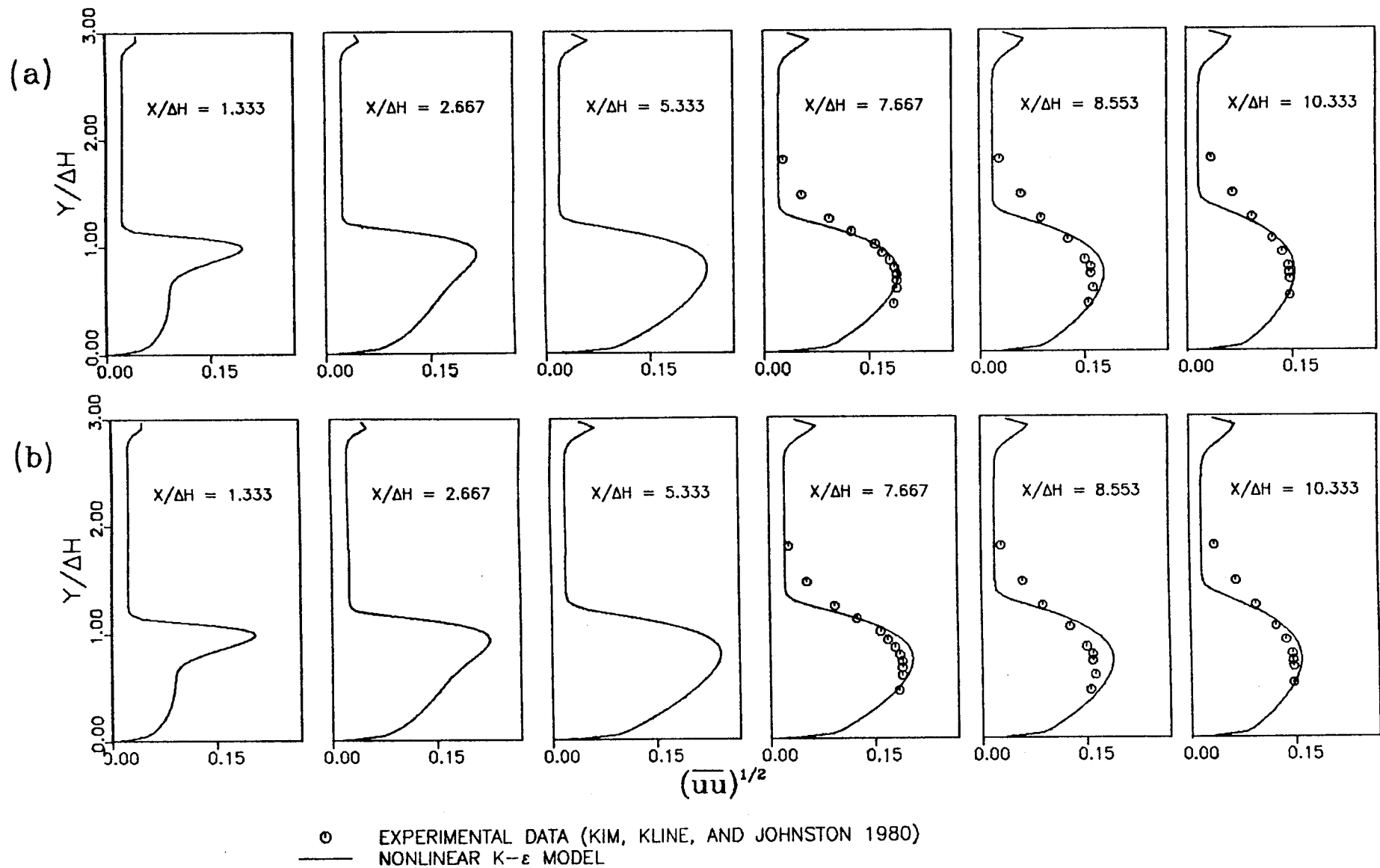


FIGURE 14. Turbulence intensities obtained from the nonlinear K- $\epsilon$  model:  
 (a)  $C_D = C_E = 1.40$  and (b)  $C_D = C_E = 1.68$

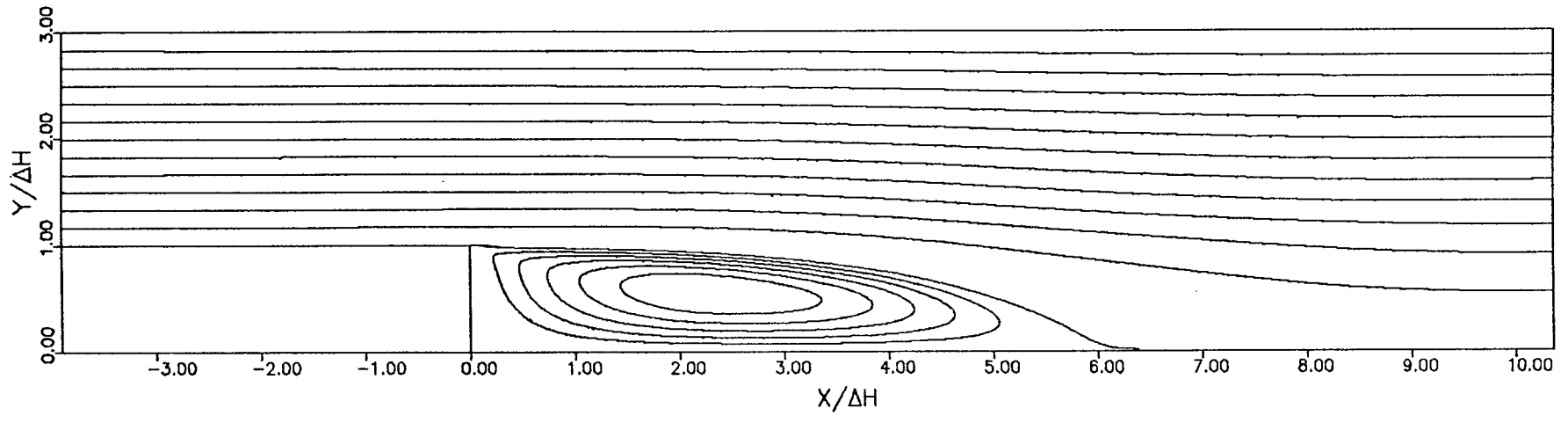
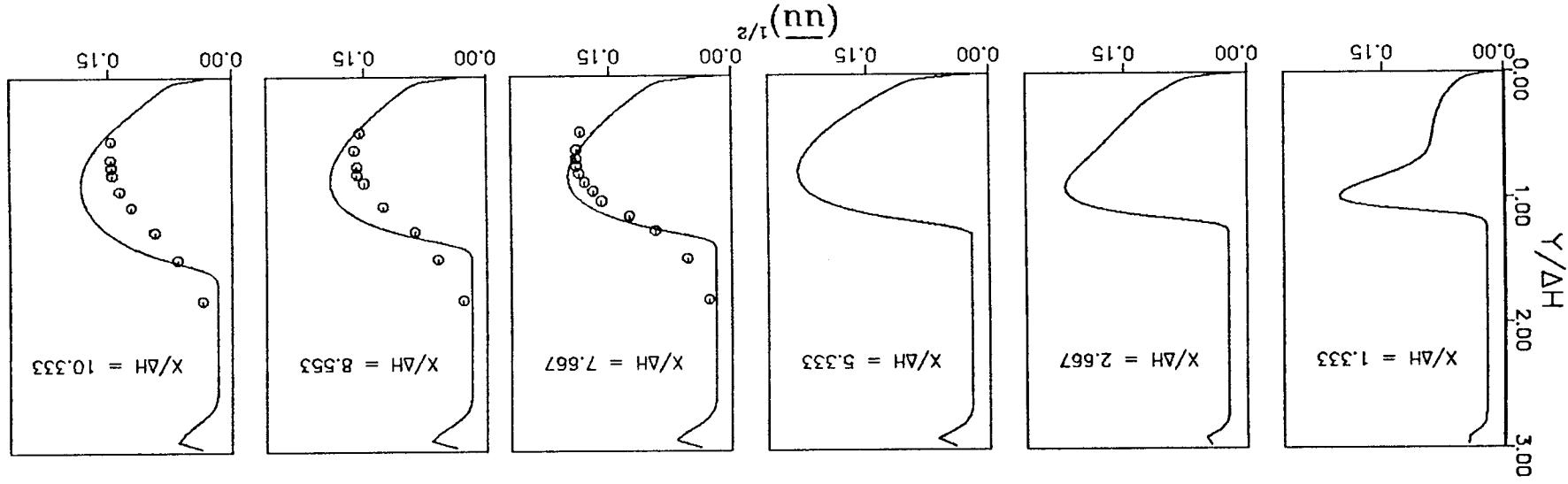


FIGURE 15. Computed streamlines obtained for the nonlinear  $K-\epsilon$  model without the second derivative terms.



○ EXPERIMENTAL DATA (KIM, KLINE, AND JOHNSTON 1980)  
 — NONLINEAR  $K-\epsilon$  MODEL

FIGURE 16. Dimensionless turbulence intensities for the nonlinear  $K-\epsilon$  model without the second derivative terms.





1. Report No. NASA CR-178421 ICASE Report No. 87-74		2. Government Accession No.		3. Recipient's Catalog No.	
4. Title and Subtitle NUMERICAL SOLUTION OF TURBULENT FLOW PAST A BACKWARD FACING STEP USING A NONLINEAR K-ε MODEL				5. Report Date December 1987	
				6. Performing Organization Code	
7. Author(s) C. G. Speziale and Tuan Ngo				8. Performing Organization Report No. 87-74	
				10. Work Unit No. 505-90-21-01	
9. Performing Organization Name and Address Institute for Computer Applications in Science and Engineering Mail Stop 132C, NASA Langley Research Center Hampton, VA 23665-5225				11. Contract or Grant No. NAS1-18107	
				13. Type of Report and Period Covered Contractor Report	
				14. Sponsoring Agency Code	
12. Sponsoring Agency Name and Address National Aeronautics and Space Administration Langley Research Center Hampton, VA 23665-5225					
15. Supplementary Notes Langley Technical Monitor: Submitted to the ASME J. Richard W. Barnwell Applied Mech.  Final Report					
16. Abstract The problem of turbulent flow past a backward facing step is important in many technological applications and has been used as a standard test case to evaluate the performance of turbulence models in the prediction of separated flows. It is well known that the commonly used K-ε (and K-l) models of turbulence yield inaccurate predictions for the reattachment point in this problem. By an analysis of the mean vorticity transport equation, it will be argued that the intrinsically inaccurate prediction of normal Reynolds stress differences by the K-ε and K-l models is a major contributor to this problem. Computations using a new nonlinear K-ε model (which alleviates this deficiency) are made with the TEACH program. Comparisons are made between the improved results predicted by this nonlinear K-ε model and those obtained from the linear K-ε model as well as from second-order closure models.					
17. Key Words (Suggested by Author(s)) turbulent flow, backward facing step, K-ε models, separated flow			18. Distribution Statement 34 - Fluid Mechanics and Heat Transfer  Unclassified - unlimited		
19. Security Classif. (of this report) Unclassified		20. Security Classif. (of this page) Unclassified		21. No. of pages 45	22. Price A03